

# The investigation of fly ash based asphalt binders using atomic force microscope

Rajan SAHA\*, Kyle MALLOY, Emil BAUTISTA, Konstantin SOBOLEV

*Department of Civil and Environmental Engineering, University of Wisconsin at Milwaukee, WI 53705, USA*

*\*Corresponding author. E-mail: rajan.saha13@gmail.com*

© Higher Education Press and Springer-Verlag Berlin Heidelberg 2017

**ABSTRACT** Atomic Force Microscope (AFM) is a relatively new technique for investigation of construction materials. In this study AFM was used to investigate the interaction of asphalt binder with fly ash. Fly ash is a coal combustion byproduct of electric power utilities having pozzolanic properties and commonly used in Portland cement concrete. In this study, an investigation was made by using different types of fly ash with two types of asphalt binders such as PG 58-28 and PG 64-28. Asphalt microstructure is divided into four subgroups such as Saturates, Aromatics, Resins and Asphaltenes (SARA). These four phases can be distinguished by the atomic force microscope. The interaction of these phases affected by introducing fly-ash was investigated and correlation with rheological properties was observed.

**KEYWORDS** AFM, fly ash, bee, rheology, asphalt

## 1 Introduction

The use of asphalt dates back thousands of years, when it was used as a waterproofing material and sealer for cracks and joints. While it is known that asphalt is composed mostly of hydrocarbons, the knowledge of its microstructure is still incomplete [1]. Optical microscopes have been used for centuries to study materials [2], but have not been effective with asphalts due to the opaque and adhesive properties of the substance. In addition to this, the resolution of an optical microscope is about 200 nm [3] which is inadequate to reveal the details of structural buildup of the binder. A relatively new technology that could provide better insight into the microstructure of asphalt is Atomic Force Microscopy (AFM) enabling the molecular and atomic resolution [4,5].

The AFM was first used to study asphalt by Loeber [6], which resulted in the detection of different phases within the asphalt. Asphalt specimens were examined under AFM and compared to the results from Scanning Electron Microscopy, and Fluorescence Microscopy. Alternating ridges and valleys, which appear as alternating white and black bands on an AFM scan, were observed and termed by Loeber et al. as “bee” structures. The “bee” structures were symmetrically aligned with alternating dark and light

lines. Each “strip” was around 100–200 nm thick. These structures have been identified as asphaltenes [1]. This observation has been also supported by Pauli et al. [7].

A study performed at the University of Wyoming [7] involved scans of asphalt samples with varying amounts and types of paraffin waxes. The samples were also varied in thickness. It was found that most of the structuring that is observed in the sample, including the “bee” structures, is due to the interaction between the paraffin waxes and the non-wax components of the asphalt. The observed structuring occurs in non-polar asphalt fractions (oil phase), which would be expected to hold the majority of the wax-type materials. The appearance of structure patterns was correlated to wax type, wax concentration and crystallising conditions, as well as asphalt and asphalt fraction crude source.

The effect of temperature and thermal histories on asphalt bee structures was further studied by Lu et al. [8] and Nahar et al. [9]. The research by Nahar et al. involved taking AFM scans of asphalt samples at various stages during a heating and cooling cycle. It was found that the bee structures and surrounding phases melted away at temperatures above 55 °C, and reformed around 45 °C. The asphalt also exhibited a structural memory, with the bee structures forming in similar patterns after they had been melted. The maximum temperature a sample is exposed to will also change the surface structure of a

sample. The amount and size of the bee structures was observed to be contingent on the wax content of the sample, but the areas containing the bees seemed to fluctuate relative to presence of asphaltenes.

The AFM methods have been used to study the effects of aging on the micro-morphology and micro-rheology of bitumen. Rebolo [10] used AFM to conduct topography, phase and friction imaging and nano-indentation experiments on aged and unaged asphalt. It was found that the asphalt films consisted of asphaltene micelles suspended throughout a hydrocarbon matrix. The micelle structure could not be detected topographically in the unaged sample, but was detected on the aged sample. The aging process seemed to increase the size of the micelles. Eventually, the micelles formed a connected network with the hydrocarbon matrix filling in the void. There was a 50% reduction in the friction coefficient due to short term aging, but no further reduction occurred after the long-term aging. Nano-indentation confined showed that aging increased the stiffness of the sample.

The mechanical properties of asphalt were also analyzed by Dourado et al. [11]. This test involved using the AFM to make indentations on different areas of an asphalt sample in order to determine the elastic modulus. The hydrocarbon matrix, the bee structures, and the areas containing bee structures were analyzed. It was found that the areas containing bee structures had a lower elastic modulus than the surrounding matrix, with the bee structure itself having a lower elastic modulus compared to the overall area. It was concluded that the areas containing bee structures are a mixture of asphaltenes and resins, with the resins forming the bright bands of the bee structure.

The interaction of asphalt with substances representing various fillers in asphalt cement was studied using AFM by Fischer [12]. The AFM was used to measure the contact angle of asphalt on various mineral samples. In each case the peri/catana phase had a smaller contact angle than the perpetua phase indicating that the affinity of the peri/catana phase for the filler is larger than for the perpetua phase. It was also observed that the bees in the peri/catana phase were smaller in size and number (density) near the bitumen-filler interface.

The scans of aged bitumen samples were also reported by Sobolev et al. [13]. Among others results, the study reported on the effect of a nano-clay (Acti-gel) additive and simulated aging process in a pressure vessel. The scans reported by Fig. 1 revealed an increase in the area of the micelle structures, which can be correlated to increased stiffness of the samples. This provides evidence that there is a relationship between the area associated with the

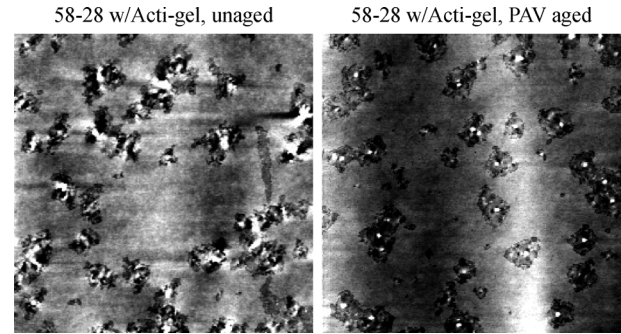


**Fig. 1** The effect of aging on the structure of bitumen binders with nano-clay, from Sobolev et al. [13].

micelle structures and the stiffness of the asphalt sample. This reported research evaluates the effects of different types of fly ash on nano-structure of asphalt binders.

## 2 Materials and sample preparation

Two different types of asphalt binders, PG 58-28 and PG 64-28, were used in this study for each type of asphalt. Different samples were produced with three different types of fly ash at three different concentrations. The specimens were designed with fly ash at content of 5%, 15% and 25% by volume. The PG 64-28 binder has higher stiffness than PG 58-28. Fly ash was mixed with asphalt using a low shear mixer at 1300 rpm. Asphalt microstructure is divided into four subgroups: saturates, aromatics, resins and asphaltenes (SARA). These four subgroups can be effectively distinguished by atomic force microscope as different phases. Table 1 shows the description and the chemical compositions of SARA.

Asphaltenes impart high viscosity to crude oils resulting in increased stiffness of the asphalt binder, which negatively impacts production and causes a number of problems in production. This model demonstrates how asphaltene molecules are dispersed in resins. Both asphaltene and resins are dispersed throughout the oil and aromatic portions of the asphalt. The asphalt binders PG 58-28 and PG 64-28 were collected from local vendors.

Fly ash is divided into two classes: C and F. When the sum of  $\text{SiO}_2$ ,  $\text{Al}_2\text{O}_3$ , and  $\text{Fe}_2\text{O}_3$  make up more than 50% of a fly ash specimen, it is considered as class C (Table 2). When the same components make up 70% of the fly ash, it is considered class F. Fly ash WE05 class C, WE07 class F, and WE08 class C were supplied by WE Energies (WI, USA) [13–15].

The most important factor in microscopic observations

**Table 1** Chemical composition of asphalt [1]

saturates	aromatics	resins	asphaltenes
n- and iso- alkanes (simple and least reactive hydrocarbon)	a type of hydro-carbon which has alternating double and single bonds between carbon atoms forming rings	viscous liquid	carbon, hydrogen, nitrogen, oxygen, and sulfur as well as trace amounts of vanadium and nickel

**Table 2** Chemical composition of fly ash [13]

materials ID	class	chemical composition, %									
		Al <sub>2</sub> O <sub>3</sub>	CaO	Fe <sub>2</sub> O <sub>3</sub>	SiO <sub>2</sub>	MgO	Na <sub>2</sub> O	K <sub>2</sub> O	TiO <sub>2</sub>	P <sub>2</sub> O <sub>3</sub>	SO <sub>3</sub>
WE05	C	22.3	24.6	5.4	32.9	6.3	2.8	0.5	1.3	1.6	1.8
WE08	C	23.9	23.1	4.5	34.4	5.3	2.2	0.6	1.3	1.5	2.1
WE07	F	27.2	5.0	14.0	45.6	1.0	0.7	1.8	1.1	0.5	2.7

of asphalt and asphalt binders is sample preparation. Asphalt has a high viscosity at ambient temperatures and high temperature sensitivity. Glass slides were used for sample preparation. Initially, the asphalt binder was placed in the oven at 130 °C for 60 minutes to lower the viscosity to a point where it can be sampled. A small drop of asphalt was then placed on the slide. The glass slide with the asphalt drop was placed in the oven for 1 minute. During this step, the asphalt drop spreads out equally and forms a very thin layer. Heat cast samples were used due to the fact that solvent cast (by using solvent with asphalt) samples did not show any bee structures.

An atomic force microscope 5420 AFM from Agilent Technologies was used in this study. The AFM used a very small silicon cantilever (type PPP-NCH) with frequency 300 kHz to scan the surface of the sample. The change in height of the sample is captured by a photo-diode which measures the position of a laser beam reflected off the back of the cantilever arm during the scan. Usually the cantilevers consisted of a macro scale rectangular base, a long, thin arm, and a fine tip. The images were of 20 μm × 20 μm size recorded in non-contact mode.

### 3 Results and discussion

All of the images were analyzed using Gwyddion software,

which was developed specifically for AFM scans. The program allows for viewing scans as a 2D or 3D image. Fig. 2 provides examples of scans of both asphalt types with 5% of fly ash.

These scans demonstrate how the “bee” structures form the spikes in the vertical direction. It also appears that spikes can form multiple ridges which look like the classical “bee” structure, as seen in the PG64-28 asphalt, or these can exist as solitary spikes, as shown for the PG58-28 asphalt. The type of crystal structure seems to be related to the type of asphalt, and is not affected by the presence of fly ash.

The Gwyddion software was used to measure two specific aspects of the crystal formation (Fig. 3). The first was the height of the crystals, which in this case meant measuring the peak crystal height in the scan which consisted of strictly the catana phase. The second method would involve measuring the overall area occupied by the crystals, which defines the catana phase and the peri phase.

These areas were selected using a tool in Gwyddion that allows the user to select areas based on height threshold. The height threshold was adjusted to select the cells. This was possible due to the cells being slightly lower than the rest of the area on the scan. After the areas were selected, the height and area calculations were executed by a statistical analysis tool in Gwyddion, which provides the data on the area selected. All analyzed scans are reported by Figs. 4 and 5.

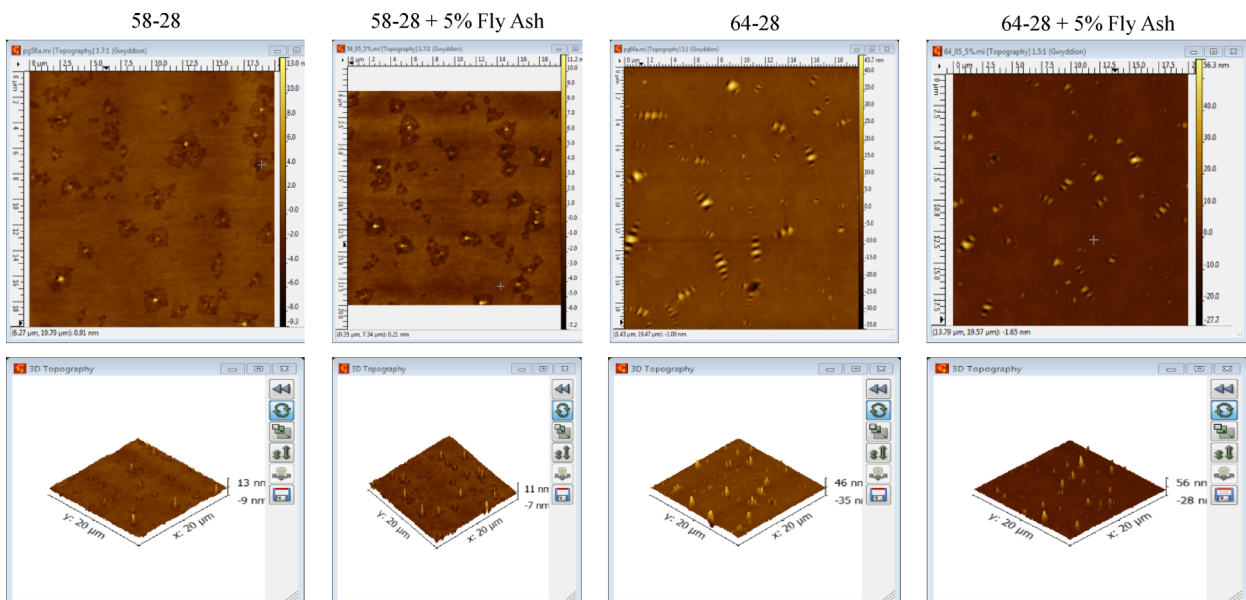


**Fig. 2** The 2D and 3D images of PG58-28 and PG64-28 binders and effect of adding of 5% fly ash

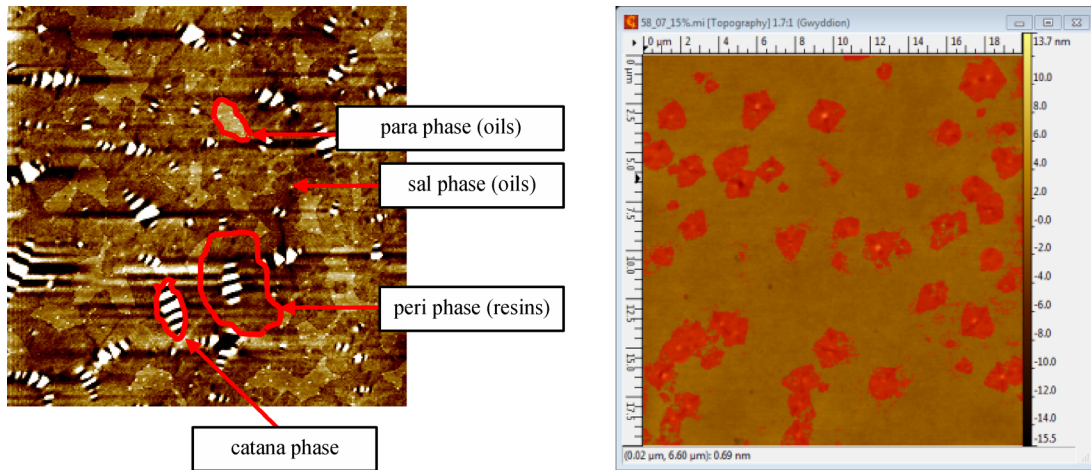


Fig. 3 The asphalt phases detected by AFM and small area analyzed by Gwyddion

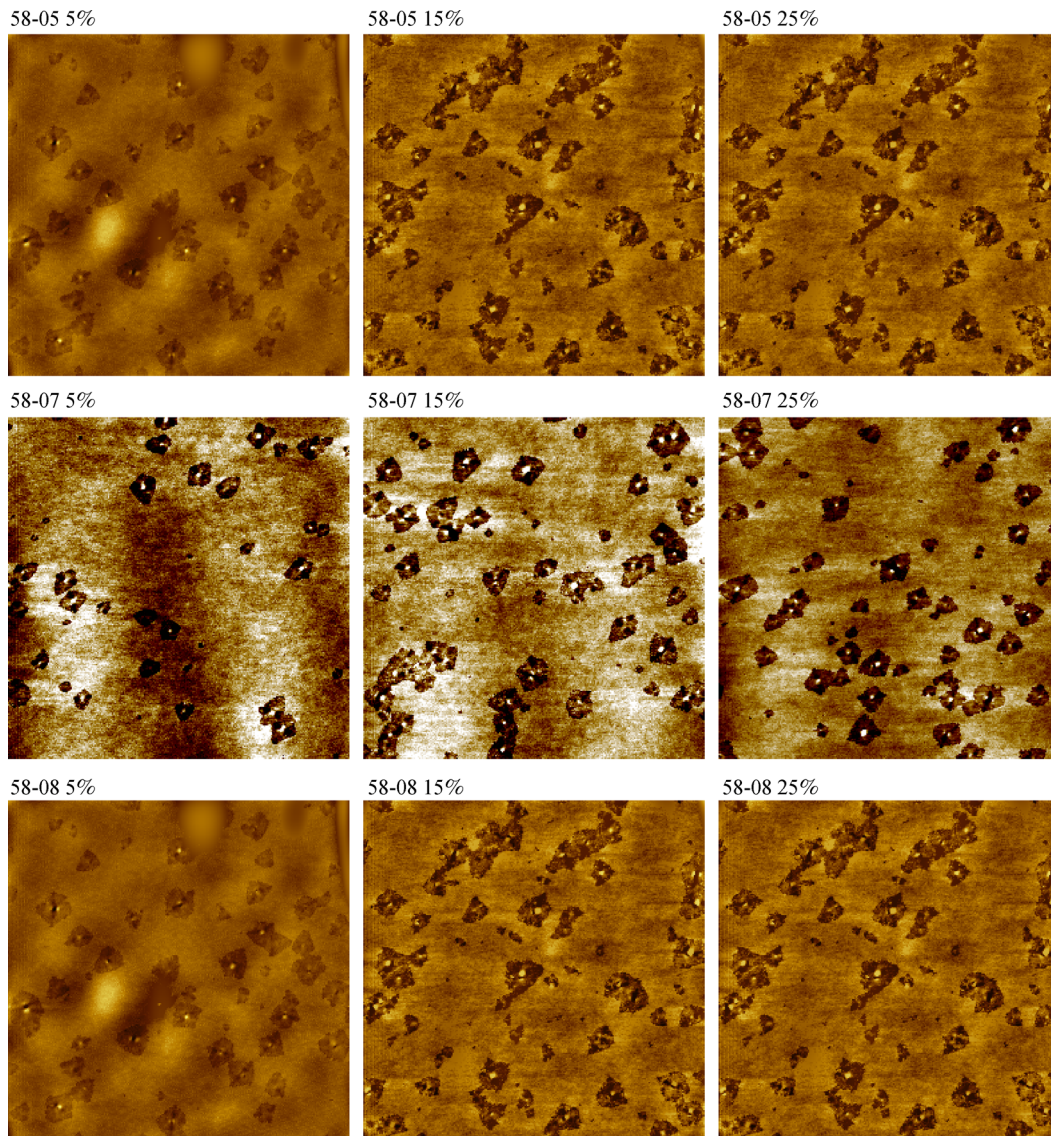
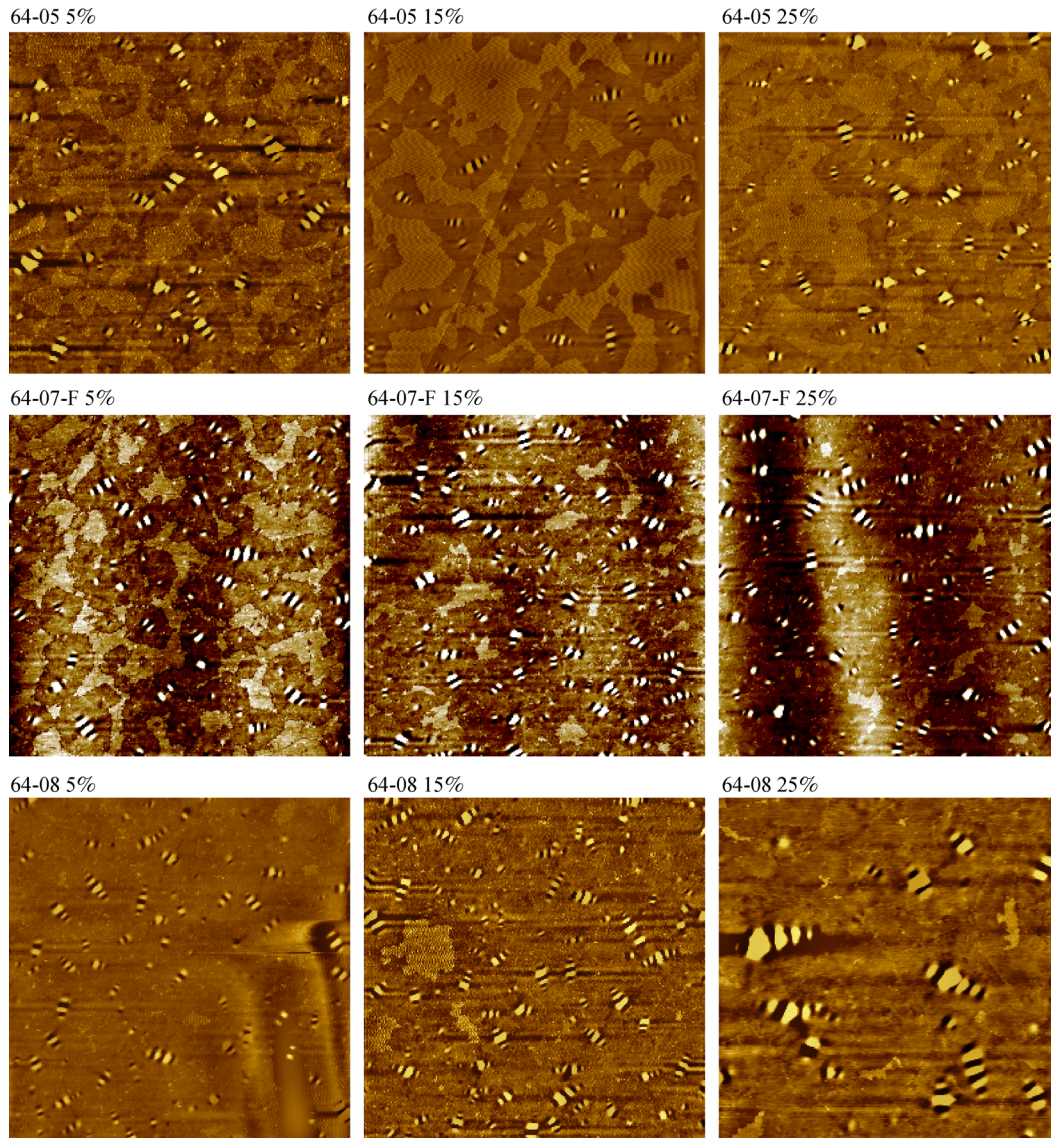


Fig. 4 The AFM scans of PG58-28 based mastics



**Fig. 5** The AFM scans of PG64-28 based mastics

The test results and the height of crystals proved no correlation between the volume of fly ash added (Fig. 6). The most of the peaks were in the 10-15 nm range with higher peaks observed on the PG64-28 samples. This was most likely due to the variation in source of the asphalt. According to Pauli et al. [16], “bee” structure crystal height correlates with the wax content.

The surface area calculations demonstrated a slight increase in the catana and peri phase area for specimens with higher content of fly ash (Fig. 7). Masson et al. [1] found a strong correlation between the size of the cell structures and the presence of nickel and vanadium and so the presence of these elements in fly ash might contribute to the increased area of the peri phase. Fly ash may have also provided more points within the asphalt for crystal-

lization to occur. This would result in the increased area of the micelle structures.

The effects of cooling rate were also investigated and reported by Fig. 8. Samples of PG58-28 mixed with 5%, 15%, and 25% fly ash were produced. Two duplicate samples were produced at each concentration of fly ash. From these, one sample was allowed to cool at a room temperature, while the other was quenched at  $-10^{\circ}\text{F}$  in a freezer.

It appears that the quenched samples formed micelle structures that are smaller in size, but greater in numbers. The surface area occupied by the micelle structures increased with fly ash content in both the room-cooled and the quenched samples. In the quenched samples, the components of the micelle structure were not able to

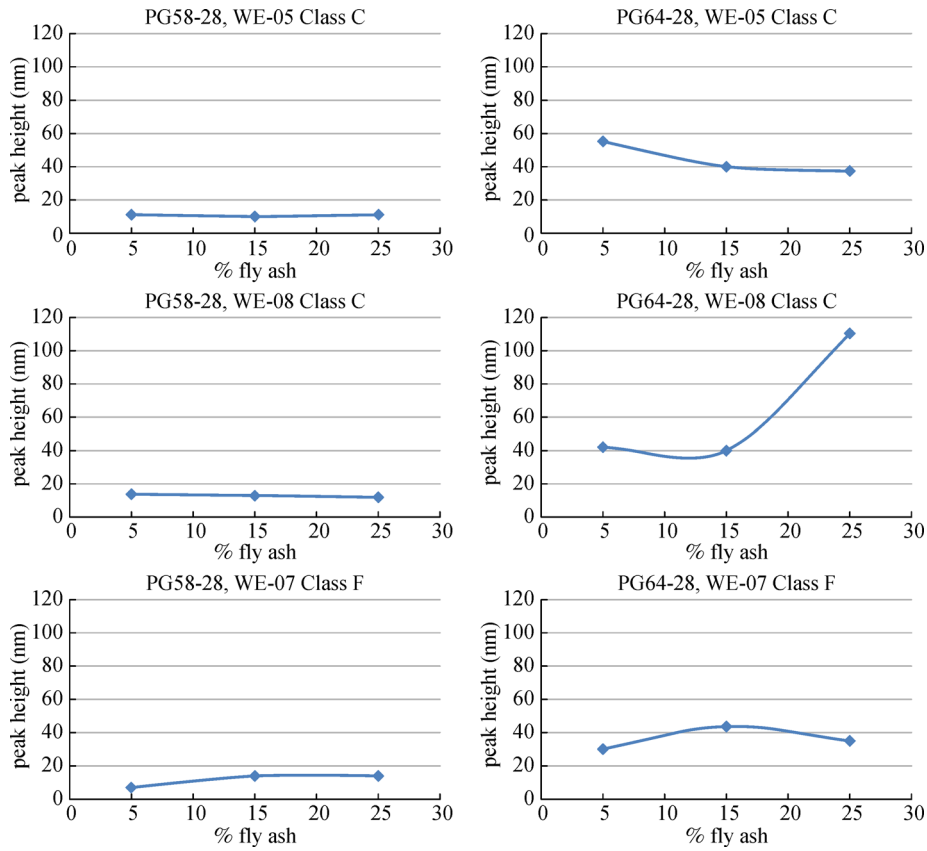


Fig. 6 The effect of fly ash on crystal height as recorded by AFM

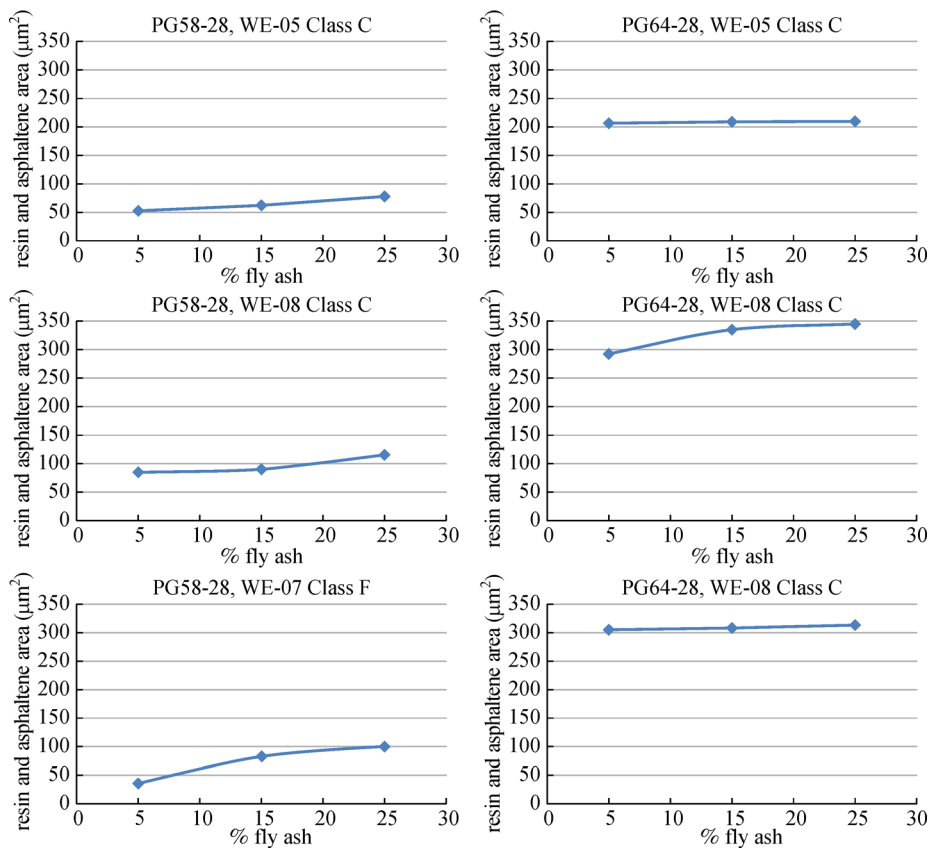
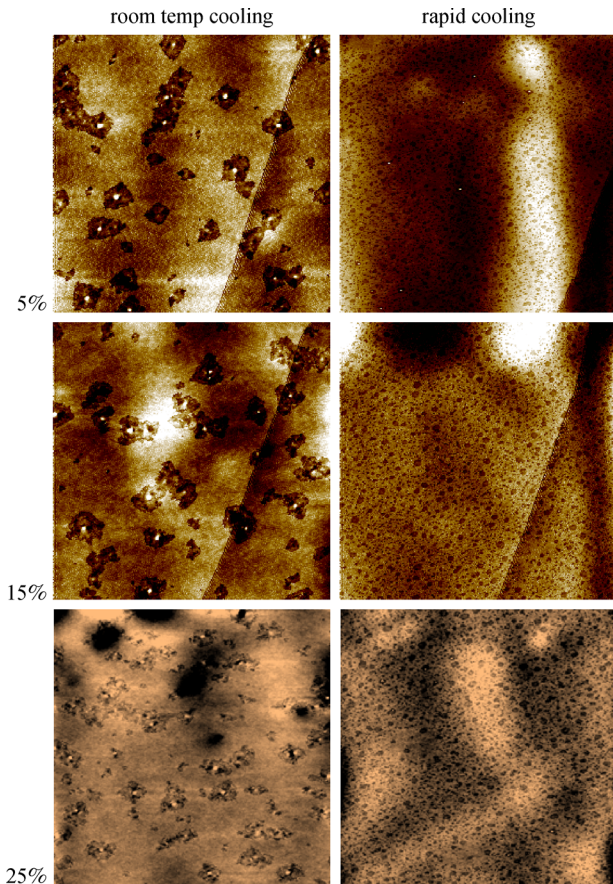


Fig. 7 The effect of fly ash on resin and asphaltene area as measured by AFM



**Fig. 8** The effect of cooling on structure of asphalt- fly ash mastic

aggregate into larger structures and so were preserved in place.

The complex modulus of each sample was measured to assess the correlation between the structure of bitumen the rheological response, and the effect of the addition of fly ash. There was a strong positive correlation between the presence of fly ash and the complex modulus.

This relationship between the complex modulus and the micelle area of a scan was analyzed. It was found that there was a positive relationship between the area of micelle structures and the stiffness of a sample. One possible conclusion is that the micelle structures provide stiffness to the sample, while the oils they are suspended in provide flexibility. An increase in the area of the micelle structures due to an increase in fly ash would result in a higher complex modulus. The results for each sample are show in Fig. 9.

#### 4 Conclusions and further research

The Atomic Force Microscope can be used to reveal the structure of bitumen with fly ash additives. The micelle structures were isolated and analyzed with the help of

Gwyddion software. The peak height and the surface area of the micelle structures were measured. No correlation was found between the fly ash content and the height of the peaks. It was found that the addition of fly ash can increase the area of the micelle structures. However, it was found that the complex modulus increased with the addition of fly ash and the area of the micelle structures. This can be interpreted that the micelle structures contribute to the stiffness of an asphalt sample.

Further research can focus on the investigation of the effect of fly ash particles on the formation of large bumps on the surface. Fly ash particles are relatively large and so must be easily detectable on the slides. A thinner sample may be required in order to investigate the effect of fly ash distributed within the sample.

**Acknowledgements** The authors acknowledge the financial support of the Energy and Power Research Institute. The support from WE Energies and Advanced Analytical Facility at University of Wisconsin-Milwaukee is appreciated.

#### References

1. Masson J, Leblond V, Margeson J. Bitumen morphologies by phase-detection atomic force microscopy. *Journal of Microscopy*, 2006, 221(1): 17–29
2. Baker H. *The microscope made easy*. Lincolnwood, IL: Science Heritage Ltd., 1987.
3. Morris V, Kirby A, Gunning A. *Atomic force microscopy for biologists*, London: Imperial College Press, 1999.
4. Binnig G, Quate C, Gerber C. *Atomic force microscope*. The American Physical Society, pp. 930–934, 1986.
5. Mou J, Sheng S, Ho R, Shao Z, Czajkowsky D. High resolution surface structures of E. coli GroES oligomer by atomic force microscopy. *FEBS Letters*, 1996, 381(1-2): 161–164
6. Loeber L, Sutton O, Morel J, Valleton J, Muller G. New direct observations of asphalts and asphalt binders by scanning electron microscopy and atomic force microscopy. *Journal of Microscopy*, 1995, 182(1): 32–39
7. Pauli A, Grimes R, Beemer A, Turner T, Branthaver J. Morphology of asphalts, asphalt fractions and model wax-doped asphalts studied by atomic force microscopy. *International Journal of Pavement Engineering*, 2011, 12(4): 291–309
8. Lu X, Langton M, Oloffson P, Redelius P. Wax morphology in bitumen. *Journal of Materials Science*, 2005, 40(8): 1893–1900
9. Nahar S, Schmetts A, Scarpas A, Schitter G. Temperature and thermal history dependence of the microstructure in bituminous materials. *European Polymer Journal*, 2013, 49(8): 1964–1974
10. Rebolo L, de Sousa J, Abreu A, Baroni M, Alencar A, Soares S, Mendes Filho J, Soares J. Aging of asphaltic binders investigated with atomic force microscopy. *Fuel*, 2014, 117: 15–25
11. Dourado E, Simao R, Leite L. Mechanical properties of asphalt binders evaluated by atomic force microscopy. *Journal of Microscopy*, 2012, 245(2): 119–128

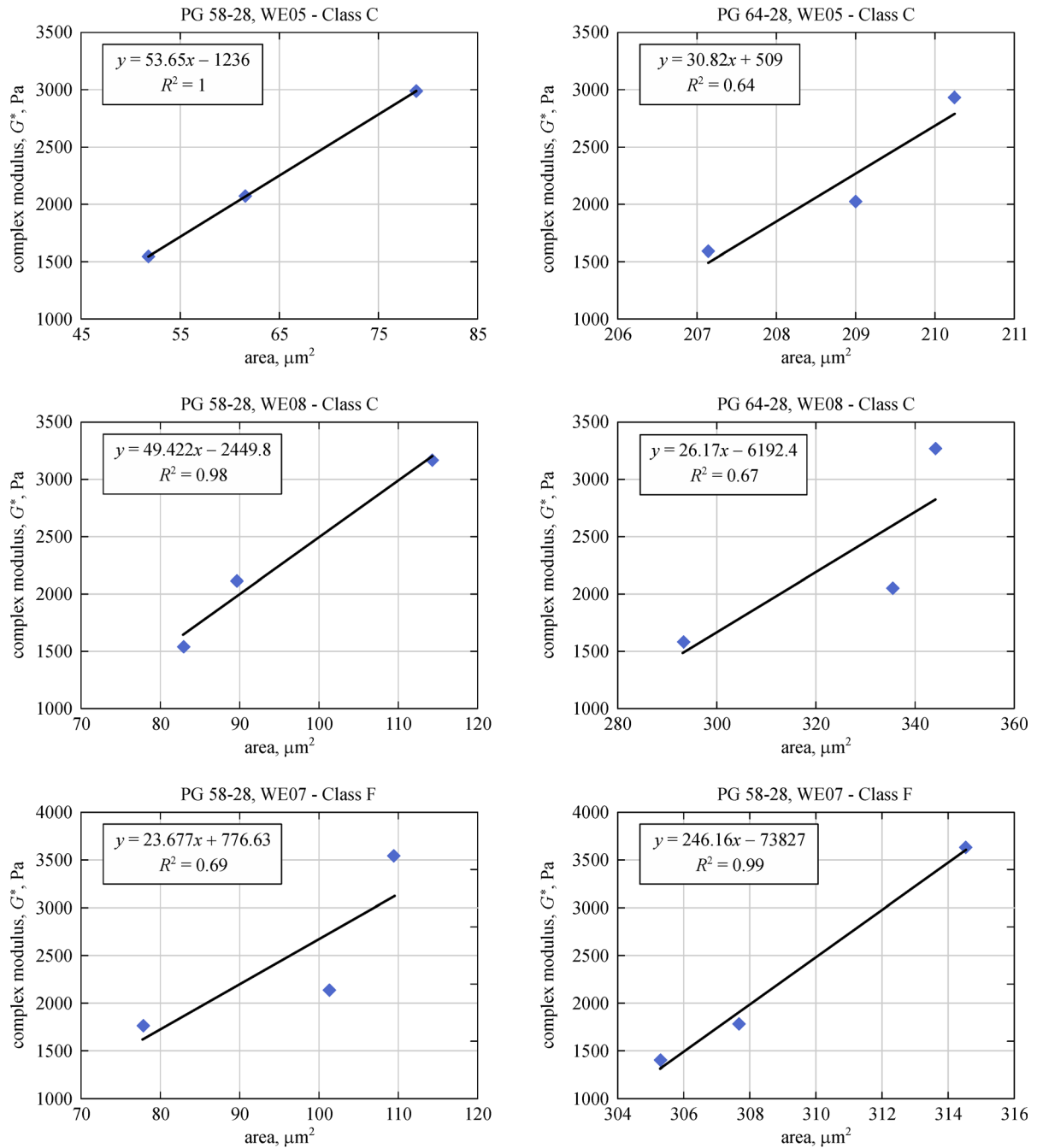


**Fig. 9** The effect of fly ash on rheological response and structure of mastics with up to 40% of fly ash

12. Fischer H R, Dillingham E, Hermse C. On the interfacial interaction between bituminous binders and mineral surfaces as present in asphalt mixtures. *Applied Surface Science*, 2013, 265: 495–499
13. Sobolev K, Flores I, Bohler J, Faheem A, Covi A. Application of fly ash in ASHphalt concrete from challenges to opportunities. We Energies, Milwaukee, WI, 2013.
14. Yu X, Burnham N A, Mallick R B, Tao M. A systematic AFM-based method to measure adhesion differences between micron sized domains in asphalt binders. *Fuel*, 2013, 113: 443–447
15. Bautista E, Flickinger J, Saha R, Flores-Vivian I, Faheem A F, Sobolev K. Effect of coal combustion products on high temperature performance of asphalt mastics. *Construction & Building Materials*, 2015, 94: 572–578
16. Pauli A T, Branthaver J F, Robertson R E, Grimes W. Atomic force microscopy investigation of SHRP asphalts. In: Symposium on Heavy oil and resid compatibility and stability, Petroleum Chemistry Division, American Chemical Society, San Diego, California, USA, 2001.